文章编号:1001 - 9014(2011)03 - 0202 - 04

Crystallization of amorphous silicon film induced by a near-infrared femtosecond laser

DAI Ye, HE Min, YAN Xiao-Na, MA Guo-Hong
(Department of Physics, Shanghai University, Shanghai 200444, China)

Abstract: 1kHz femtosecond laser was used to induce crystallization on amorphous Si film. Raman spectra show that the crystallization region depended critically on the laser fluence and profile. Furthermore, a textured surface with a mass of fine-grained crystalline Si was observed through SEM. This structure might result from the explosive crystallization and epitaxial growth of Si nucleation on the interface of liquid-solid Si. Due to the simultaneous process of crystallization and surface texturing, this laser treated region enhanced its absorbance in the visible and infrared band.

Key words: amorphous physics; crystallization; femtosecond laser; Si
PACS: 81.10.Jt, 78.66.Jg, 79.20.Ds

近红外飞秒激光诱导非晶硅薄膜的晶化

戴 晔, 何 敏, 阎晓娜, 马国宏
(上海大学 物理系,上海 200444)

摘要: 1kHz 的飞秒激光辐照在非晶硅薄膜后会使得辐照区域的薄膜产生晶化现象. 拉曼光谱表明这个激光诱导晶化过程与入射激光的能量及其模式分布有密切的联系. 扫描电镜观测发现激光辐照区域形成了粗糙的表面纹理,并且大量的晶粒形成在这个结构表面. 这个晶化现象可能是由于爆炸晶化成核和晶粒外延生长共同作用的结果,进一步的研究表明这种飞秒激光诱导的晶化结构能够增进该薄膜在可见和红外波段的光学吸收.

关 键 词: 非晶态物理; 晶化; 飞秒激光; 硅
中国分类号: O434.3 **文献标识码**: A

Introduction

Recently femtosecond laser-induced space-selective microstructure changes or crystallization in materials have attracted much attention because laser fabrication is a one-step technique compared with the conventional photolithography methods[1,2]. In the previous studies, the nonlinear optics crystals have been induced in glass using 250kHz femtosecond laser, which could be due to the heat accumulation effect[3,4]. The crystallization characteristics of some film materials, e.g., amorphous silicon (a-Si) and GeSb, during the 1 kHz femtosecond laser irradiation process have also been intensively studied in past decades[5~8]. However, for either 1 kHz or 250kHz, the mechanisms of femtosecond laser-induced crystallization are still not fully understood up to date. Especially for the a-Si film, the spatially selective crystallization using femtosecond laser irradiation could construct a poly-silicon matrix on a flexible substrate. Thus it has potential application in fabrication of thin film transistors (TFTs) and solar cell matrix (SCM)[9]. Therefore, the research on femtosecond laser-induced crystallization of a-Si film will greatly promote development of this technique. In this paper, we explored femtosecond laser-induced crystallization process on a-Si film using a

Received date: 2010 - 08 - 30, **revised date**: 2010 - 11 - 17 **收稿日期**:2010 - 08 - 30, **修回日期**:2010 - 11 - 17
Foudantion item: Supported by National Nature Science Foundation of China (60908007, 10774099); Shanghai Oriental Scholars Program (09530501100); Shanghai Leading Academic Discipline Project (S30105)
Biography: Dai Ye (1980-), male, Jiangsu, China, research field is femtosecond laser interaction with condensed matter. E-mail: yedai@shu.edu.cn.

800nm near-infrared femtosecond laser. Micro-Raman spectroscopy showed that the size of crystallization region depended highly on the laser fluence and profile. In addition, there exhibited a kind of textured microstructure on the irradiated surface, and thus two amorphous and microcrystalline phases of this composite structure could result in the enhancement of its optical absorption in the visible and infrared band. We suggest that this technique could be applied for fabrication of the solar energy cell or sensor.

1 Experimental

The sample used in this study was a thin layer of a-Si deposited onto a SiO_2 glass substrate by PECVD technique. The thickness of the a-Si layer was 100nm. A regenerative amplified Ti: Sapphire mode-locked pulse laser (Spitfire, Spectra-Physics Co.) emits a train pulse of 1kHz, 120fs and 800nm. A Gaussian profile laser beam was guided onto the film by a 20 × objective lens (N. A. = 0.3), and the size of the focused point was about 10μm in the focal point. With the help of an XYZ stage, we could select the irradiated region by moving the laser focal point. A computer-controlled electronic shutter was inserted into the optical path in order to determine the laser pulse number irradiated on the samples. The average power of incident laser could be controlled by adjusting a neutral density filter. Micro-Raman spectroscopy (Renishaw Invia) with 785nm light excitation and SEM (JSM-6700F) were carried out on the laser treated/untreated surfaces to study the crystallization process induced by the femtosecond laser irradiation. The optical absorptions of the sample before and after femtosecond laser irradiation were measured using a Jasco V-570 spectrophotometer at room temperature.

2 Results and discussion

Figure 1 shows the morphology evolution of the irradiated surface after 1, 10, 100, 1000 and 5000 pulses, which mean that the shutter's opening times were 1 ms, 10 ms, 100 ms, 1 s and 5 s respectively. The energy of the incident pulse was about 1μJ. In this image, after a single pulse irradiation, the center in the irradiated surface changed to black from ruby, and the diameter of the irradiated surface was about 10μm, which was approximate to the laser focal size. Meanwhile, as a result of femtosecond laser-induced plasma micro-explosion, some structure deformation or defects due to the non-thermal shock appeared in the laser-affected zone. In figure 1, a gray circle with some ripples occurred in the outskirt of the black region, which mostly resulted from the induced lattice distortion and non-thermal phase transition of a-Si film. With the number of the incident pulse increasing, the black region gradually shrank due to the repeated laser ablation, and the laser-affected zone diffused to the neighbour region. After thousands of pulses, the a-Si film in the focal center became less and less to the extent that the glass substrate was uncovered. These phenomena indicated that a small quantity of femtosecond laser pulses might induce the structural changes in the a-Si film, but the film would be destroyed if the laser fluence exceeded its ablation threshold.

In order to study the black region on a-Si film, a micro-Raman spectroscopy was used to examine the irradiated surface. Firstly, as shown in figure 2 (a), a black region was induced by a single femtosecond laser with 1μJ on a-Si film, and the corresponding Raman curve was displayed in figure 2(b). Meanwhile, the Raman spectra of the a-Si film and the single crystal Si were also displayed in figure 2(b) for comparison. As we know, a peak at 520cm^{-1} is associated with the transverse optic phonon mode of single crystal Si, and the peak at around 480cm^{-1} is associated with the a-Si phase[10]. According to these spectra, the black region in the focused center had partially changed to microcrystalline silicon due to the obvious Raman peak at 517cm^{-1}, but the neighbour zone without irradiation

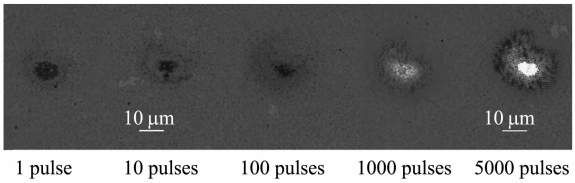

Fig. 1　The image of the irradiated surfaces after 1, 10, 100, 1000, 5000 pulses respectively. The white bars in the image denote 10μm

图 1　非晶硅薄膜分别经过 1, 10, 100, 1000, 5000 个飞秒激光脉冲辐照后的光学显微照片. 白色标尺表示 10μm

still remained a-Si phase. Therefore, these results indicated that the amorphous phase could transform to the crystalline phase after femtosecond laser irradiation. Furthermore, a Raman mapping was employed to analyze the femtosecond laser-induced microcrystalline silicon distribution around the focal point. In figure 2 (c), the Raman intensity of the peak at 517cm^{-1} was selected to construct a contour map. It showed that the Raman intensity gradually weakened from the center to the outsides. This map is similar to a Gaussian laser intensity distribution. Moreover, it is believable that the 517cm^{-1} Raman peak represents the induced microcrystalline Si. Therefore, the crystallization distribution was highly associated with the laser profile and fluence. Otherwise, the a-Si crystallization rate X_c can be calculated by the equation[11]: $X_c = \frac{I_c}{I_c + I_a}$, where I_C is integrated crystalline intensity of the area under the 520cm^{-1} peak and I_a is the integrated amorphous intensity of the area under 480cm^{-1}. After calculation, the crystallization rate X_c in the center is about 26.7%. This result is acceptable taking into account the coexistence state of two-phase a-Si and μc-Si.

We also used SEM to observe the femtosecond laser induced black region. The images in figure 3(a), corresponding to the laser fluence of 127mJ/cm^2, show some significant structure changes in the black region. From the figure 3(b), the irradiated surface became obviously roughened and some textured nanostructures occurred. This situation possibly resulted from the thermal melting and resolidification of the a-Si film. Followed by this assumption, after femtosecond laser irradiation, electron-hole plasma would rapidly quench, and a liquid phase floated and propagated on the surface layer. Due to the heat loss via rapid diffusion, a textured structure formed during the subsequent solidification process. Besides, we also found many particles with the size of nanometer-scale adsorbed on the spikes in figure3(c). According to the so-called explosive crystallization mechanism[12], we speculate that these particles should be the polycrystalline Si because the nucleation takes place most likely near the interface of liquid-solid Si from an undercooled liquid Si layer. However, the portion of the polycrystalline Si

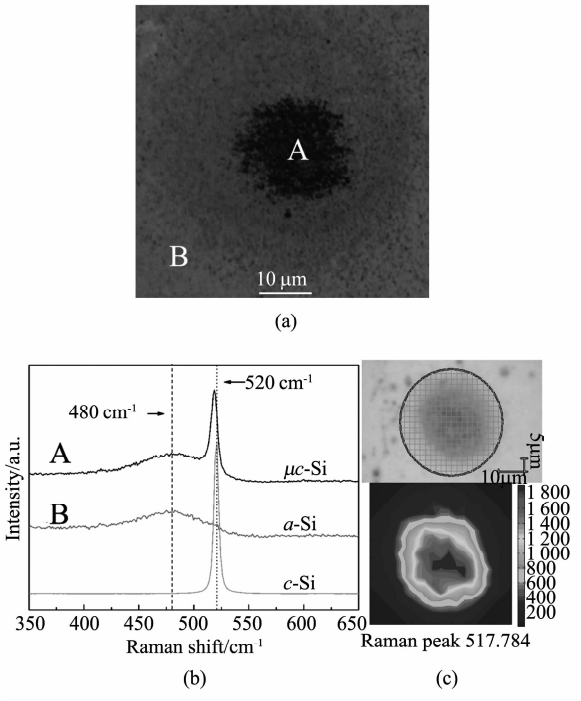

Fig. 2 (a) An image of the femtosecond laser irradiated surface (b) the Raman spectra of the black region (A) and the a-Si film (B) (c) a mapping picture of the Raman intensity with peak at 517 cm^{-1}. The color column represents the magnitude of Raman intensity. The white bars in the image (a) denote 10μm

图 2 (a)非晶硅薄膜经过 1 个飞秒激光脉冲辐照后的光学照片 (b)辐照区域不同部位的拉曼光谱 (c)拉曼峰位在 517cm^{-1}信号强度分布图. 白色标尺表示 10μm

is so few that it can not satisfactorily explain the current crystallization rate (more than 20percent). Therefore, we think that the melted crystallization might be another possible crystallization mechanism in this instance. It means some fine-grained crystalline Si might grow up in the nucleation sites and then continue their epitaxial growth on thermal melting layer.

Since the crystallization region on the a-Si film became black after femtosecond laser irradiation, we studied its optical absorption changes using a spectrophotometer. Here we used femtosecond laser to directly write a 3×3mm^2 crystallization region, as shown as the inset in figure 4. Although the irradiated surface was not so uniform, the black area still accounted for nearly 80% of the entire scanning region. Figure 4 shows the absorbance difference of the a-Si film before and after femtosecond laser irradiation. It is obvious that the laser treated region could significantly enhance the absorption in visible and infrared band. Compared with

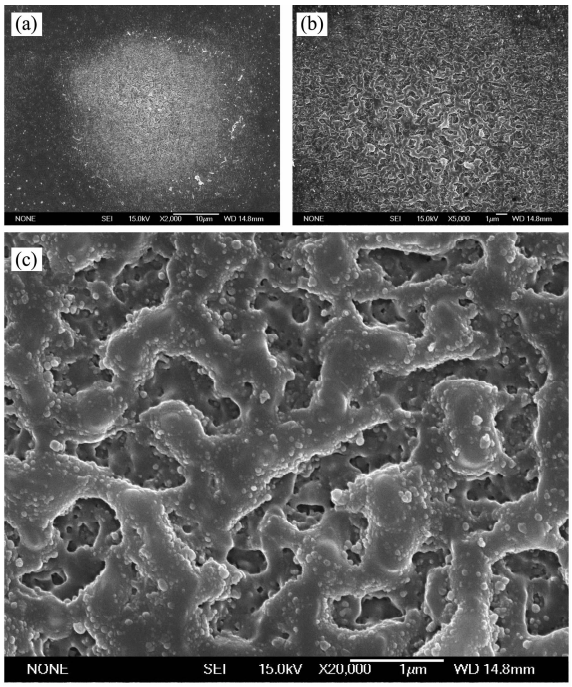

Fig. 3　SEM images of crystallization of a 100nm thick a-Si film irradiated by a single femtosecond laser pulse at fluence of 127mJ/cm^2. (a) The whole irradiated region; (b) ×5 000; (c) ×20 000

图 3　非晶硅薄膜在飞秒激光辐照强度大约为 127mJ/cm^2 后的电镜照片. (a) 全图; (b) 放大 5 000 倍; (c) 放大 20 000倍

the as-grown a-Si film, the textured surface could readily trapped the incident light into these irregular cavities where the light energy was gradually absorbed and dissipated through multiple reflection. Hence, this femtosecond laser induced crystallization process along with the surface texturing could enhance light absorption of a-Si film. This technique can be applied in fabrication of thin film transistors and improving the absorption efficiency of solar cell.

3　Conclusion

A space-selective crystallization on amorphous silicon film was achieved by controlling an 800nm near infrared femtosecond laser. Raman spectra indicated that a phase transition from a-Si to microcrystalline Si was conducted in the focused region, and the size of crystallization region depended highly on the laser influence and profile. By SEM observation, we found that a mass of fine-grained crystalline Si appeared on the textured surface. They could have been resulted from the epitaxial growth of Si nucleation on the interface of liquid-solid Si. Further, the absorption spectra showed that this kind of crystallization structure might enhance its absorbance in the visible and infrared band. Because of the simultaneous process of crystallization and surface texturing, we suggest that this technique could be applied for fabrication of TFT, solar energy cell or sensor.

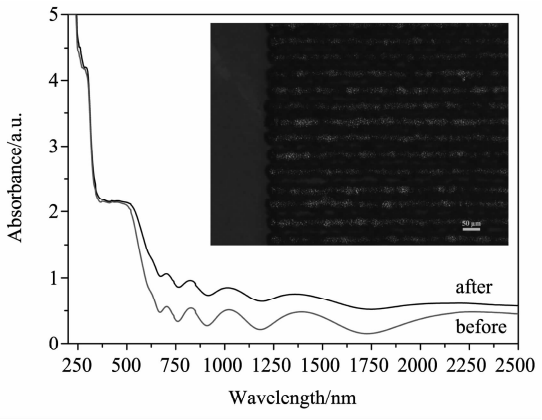

Fig. 4　Absorbance of a-Si film before and after femtosecond laser irradiation. The inset is the optical image of a-Si film. The green bar denotes 50μm

图 4　非晶硅薄膜在飞秒激光辐照后的吸收光谱变化. 插入图是辐照区域的光学照片, 其中标尺表示 50μm

REFERENCES

[1] HER T, FINLAY R, WU C, *et al*, Microstructuring of silicon with femtosecond laser pulses[J]. *Applied Physics Letters*, 1998, **73**(12): 1673—1675.

[2] LI Yan, GUO Heng-Chang, AN Ran, *et al*. Micro/Nanofabrication of condensed matters by near infrared femtosecond laser pulses, *J. Infrared Millim. waves*(李焱, 郭亨长, 安然, 等. 凝聚态物质的近红外飞秒激光微纳制备, **红外与毫米波学报**)[J]. 2005, **24**(3): 182—184.

[3] MIURA K, QIU J, MITSUYU T, *et al*. Space-selective growth of frequency-conversion crystals in glasses with ultrashort infrared laser pulses[J]. *Optics Letters*, 2000, **25**(6): 408—410.

[4] DAI Y, ZHU B, QIU J, *et al*. Direct writing three-dimensional $Ba_2TiSi_2O_8$ crystalline pattern in glass with ultrashort pulse laser[J]. *Applied Physics Letters*, 2007, **90**(18): 181109—1/3.

[5] CHOI T, HUANG D, GRIGOROPOULOS C, Ultrafast laser-induced crystallization of amorphous silicon films[J]. *Optical Engineering*, 2003, **43**(11): 3383—3388.

[6] ShIEH J, CHEN Z, DAI B, *et al*. Near-infrared femtosecond laser-induced crystallization of amorphous silicon[J]. *Applied Physics Letters*, 2004, **85**(7): 1232—1234.

[7] LEE G, PARK J, KIM E, *et al*. Microstructure of femtosecond laser-induced grating in amorphous silicon[J]. *Optics Express*, 2005, **13**(17): 6445—6453.

[8] SOKOLOWSKI-TINTEN K, SOLIS J, BIALKOWSKI J, *et al*. Dynamics of Ultrafast Phase Changes in Amorphous GeSb Films[J]. *Physical Review Letters*, 1998, **81**(17):

3679—3682.
[9] NAYAK B, EATON B, SELVAN J, *et al*. Semiconductor laser crystallization of a-Si: H on conducting tin-oxide-coated glass for solar cell and display application[J]. *Applied Physics A*, 2005, **80**(5): 1077—1080.
[10] ZHANG Shi-Bin, LIAO Xian-Bo, AN Long, *et al*. Micro-Raman study on hydrogenated protocrystalline silicon films [J]. *Acta Physica Sinica*, (张世斌, 廖显伯, 安龙, 等. 非晶/微晶过渡区域硅薄膜的微区喇曼散射研究. **物理学报**), 2002, **51**(8): 1811—1815.
[11] VOUTSAS A, HATALIS M, BOYCE J, *et al*. Raman spectroscopy of amorphous and microcrystalline silicon films deposited by low-pressure chemical vapor deposition [J]. *Journal of Applied Physics*, 1995, **78**(12): 6999—7006.
[12] MURAKAMI K, ERYU O, TAKITA K, *et al*. Explosive crystallization starting from an amorphous-silicon surface region during long-pulse laser irradiation[J]. *Physical Review Letters*, 1987, **59**(19): 2203—2206.

(上接201页)

3 Conclusion

CIGS thin films have been successfully prepared by a two-step process with solid Se powder instead of toxic H_2Se gas onto Mo-coated soda lime glass, SLG and SiO_2 substrates. It has been found that the sputtering power and substrates have a significant effect on the microstructure, surface morphology, composition, and optical performance of CIGS films. The XRD and EDS data indicate that each film has a single chalcopyrite structure, and the gallium concentration in the film increases with the increased sputtering power of precursors. The SEM pictures show that the film sputtered at 50W onto the SLG/Mo substrate exhibits a more uniform and dense surface and larger size columnar grains. The band gaps for samples obtained at the sputtering power of 50W, 60W and 70W were estimated to be 1.21, 1.23 and 1.24 eV, respectively. The fabricated CIGS films may be suitable for the application in the environmental friendly thin film solar cell.

Acknowledgements

The authors thank Prof. Zh. M. Huang, P. P. Chen, Drs. F. W. Shi, J. H. Ma, Y. F Liu, and Y. H. Zhan for their help in the experimental measurements and valuable discussions on experimental data.

REFERENCES

[1] Repins I, Contreras M A, Egaas B, *et al*. 19.9%-efficient ZnO/CdS/$CuInGaSe_2$ Solar Cell with 81.2% Fill Factor [J]. *Prog. Photovolt: Res. Appl.*, 2008, **16**: 235—239.
[2] Negami T, Hashimoto Y, Nishiwaki S. Cu(In, Ga)Se_2 thin-film solar cells with an efficiency of 18% [J]. *Solar Energy Materials & Solar Cells*, 2001, **67**: 331—335.
[3] Song Ho-Keun, Kim Soo-Gil, Kim Hyeong-Joon, *et al*. Preparation of $CuIn_{1-x}Ga_xSe_2$ Thin Films by Sputtering and Selenization Process [J]. *Solar Energy Materials and Solar cells*, 2003, **75**: 145—153.
[4] Negami T, Satoh T, Hashimoto Y, *et al*. Large-area CIGS Absorbers Prepared by Physical Vapor Deposition[J]. *Solar Energy Materials and Solar Cells*, 2001, **67**: 1—9.
[5] Fernfindez A M, Bhattacharya R N. Electrodeposition of $CuIn_{1-x}Ga_xSe_2$ Precursor Films: optimization of Film Composition and Morphology [J]. *Thin Solid Films*, 2005, **474**: 10—13.
[6] Liu Wei, Tian Jian-Guo, He Qing, *et al*. The influence of alloy phases in the precursors on the selenization reaction mechanisms [J]. *J. Phys. D: Appl. Phys.*, 2009, **42**: 1—5.
[7] Moussa G W El Haj, Ajaka M, Tahchi M. El, *et al*. Ellipsometric spectroscopy on polycrystalline $CuIn_{1-x}Ga_xSe_2$: Identification of optical transitions [J]. *Phys. Stat. Sol.* (*a*), 2005, **202**: 469—475.
[8] Dejene F B, Alberts V. Structural and optical properties of homogeneous Cu(In, Ga)Se_2 thin films prepared by thermal reaction of InSe/Cu/GaSe alloys with elemental Se vapour [J]. *J. Phys. D: Appl. Phys.*, 2005, **38**: 22—25.
[9] Venkatachalam M, Kannan M D, Jayakumar S, *et al*. Effect of annealing on the structural properties of electron beam deposited CIGS thin films [J]. *Thin Solid Films*, 2008, **516**: 6848—6852.
[10] Rockett A. The Electronic effects of point defects in $CuIn_{1-x}Ga_xSe_2$ [J]. *Thin Solid Films*, 2000, **361—362**: 330—337.
[11] Assmann L, Berne`de J C, Drici A, *et al*. Study of the Mo thin films and Mo/CIGS interface properties[J]. *Applied Surface Science*, 2005, **246**: 159—166.
[12] Shankar K, Tep K C, Mor G K, *et al*. An electrochemical strategy to incorporate nitrogen in nanostructured TiO_2 thin films: modification of bandgap and photoelectrochemical properties[J]. *J. Phys. D: Appl. Phys.*, 2006, **39**: 2361—2366.
[13] Bouabid K, Ihlal A, Manar A, *et al*. Effect of deposition and annealing parameters on the properties of electrodeposited $CuIn_{1-x}Ga_xSe_2$ thin films[J]. *Thin Solid Films*, 2005, **488**: 62—67.
[14] Lundberg O, Edoff M, Stolt L. The effect of Ga-grading in CIGS thin film solar cells[J]. *Thin Solid Films*, 2005, **480—481**: 520—525.
[15] Wei Su-Hai, Zhang S B, Zunger A. Effects of Ga addition to $CuInSe_2$ on its electronic, structural, and defect properties[J]. *Appl. Phys. Lett.*, 1998, **72**: 3199—3201.